Aerosol Science and Technology

ISSN: 0278-6826 (Print) 1521-7388 (Online) Journal homepage: https://www.tandfonline.com/loi/uast20

Friction Coefficient and Mobility Radius of Fractal-Like Aggregates in the Transition Regime

Anastasios D. Melas, Lorenzo Isella, Athanasios G. Konstandopoulos & Yannis Drossinos

To cite this article: Anastasios D. Melas, Lorenzo Isella, Athanasios G. Konstandopoulos & Yannis Drossinos (2014) Friction Coefficient and Mobility Radius of Fractal-Like Aggregates in the Transition Regime, Aerosol Science and Technology, 48:12, 1320-1331, DOI: 10.1080/02786826.2014.985781

To link to this article: https://doi.org/10.1080/02786826.2014.985781

Aerosol Science and Technology, 48:1320–1331, 2014
Published with license by Taylor & Francis
ISSN: 0278-6826 print / 1521-7388 online
DOI: 10.1080/02786826.2014.985781

Friction Coefficient and Mobility Radius of Fractal-Like Aggregates in the Transition Regime

Anastasios D. Melas,[1,2,3] Lorenzo Isella,[4] Athanasios G. Konstandopoulos,[2,3] and Yannis Drossinos[1]

[1]*European Commission, Joint Research Centre, Ispra, Italy*
[2]*Department of Chemical Engineering, Aristotle University, Thessaloniki, Greece*
[3]*Aerosol and Particle Technology Laboratory, Chemical Process and Energy Resource Institute/Centre for Research and Technology Hellas, Thessaloniki, Greece*
[4]*European Commission, Joint Research Centre, Brussels, Belgium*

The influence of geometric properties and particle size on mobility properties of fractal-like aggregates was studied in the mass and momentum-transfer transition regimes. Two methodologies were investigated. The Collision Rate Method (CRM) that determines the slip correction factor through the ratio of two fictitious Brownian particle-aggregate effective collision rates, and the Adjusted Sphere Method (ASM) that assumes the existence of a virtual, flow-independent adjusted sphere with the same slip correction factor as the aggregate over the entire transition regime. The simulated fractal-like aggregates were synthetic as they were generated via a cluster–cluster agglomeration algorithm. The CRM was used to calculate the adjusted-sphere radius of various aggregates: we found it to be weakly dependent on the monomer Knudsen number for Kn greater than 0.5. Numerical expressions for the aggregate orientationally-averaged projected area and the adjusted-sphere radius are proposed. Both expressions depend on geometric, non-ensemble averaged quantities: the radius of gyration and the number of monomers. The slip correction factor and the mobility radius of DLCA and RLCA aggregates were calculated using the ASM: for a given number of monomers, fractal dimension and prefactor, and Knudsen number their values were approximately constant (averaged over aggregate realizations). A fractal-like scaling law based on the mobility radius was found to hold. The mobility fractal dimension and prefactor were determined for different aggregates. The hydrodynamic radius, proportional to the friction coefficient, and the dynamic shape factor of DLCA and RLCA aggregates were also calculated.

1. INTRODUCTION

Over the last decades the areas of aerosol applications have significantly increased. Aerosols are used to produce high technology materials such as ceramic powders, superconducting materials, and optical fibers. By contrast, studies on combustion-generated aerosols, and more specifically soot, indicate that they may be responsible for adverse health effects (Giechaskiel et al. 2009) and climate change (Kaufman and Koren 2006). Irrespective of whether aerosol particles may be considered "desirable" or "undesirable," the study of their morphological and dynamic properties is of crucial importance.

The mobility of aerosol particles is a fundamental property as it determines their friction (Melas et al. 2014a) and diffusion (Cai and Sorensen 1994) coefficients, and it influences particle coagulation (Kostoglou and Konstandopoulos 2001). Aerosol particles may form complex structures, the calculation of their dynamic properties becoming more demanding as their structure becomes more complex. The mobility of these structures is usually expressed via the equivalent mobility radius, R_m, the radius of a virtual sphere of the same average mobility (friction coefficient) as the aerosol particle of irregular shape under the same flow conditions (Filippov 2000). The main factors that influence the mobility radius are morphology (Melas et al. 2014a) and the momentum-transfer regime, as specified by a characteristic particle length scale (Melas et al. 2014b).

The characteristic particle size L is examined relative to a characteristic medium distance, their relationship expressed via the Knudsen number, $Kn = \lambda/L$ where λ is the carrier-gas mean free path. For spherical particles L is the particle radius, while for more complex structures different lengths can be used. When the Knudsen number approaches zero particles lie in the

Received 4 July 2014; accepted 8 October 2014.

Address correspondence to Yannis Drossinos, European Commission, Joint Research Centre, Ispra, VA I-21027, Italy. E-mail: ioannis.drossinos@jrc.ec.europa.eu

Color versions of one or more of the figures in the article can be found online at www.tandfonline.com/uast.

mass/momentum continuum regime, while in the opposite limit ($Kn > 10$) they lie in the free molecular regime. Most aerosols lie in the transition regime where the characteristic length is comparable to the gas mean free path, and the Knudsen number is $0 < Kn \leq 10$.

Herein, we consider fractal-like aggregates composed of non-overlapping, touching, spherical monomers of radius R_1. The friction coefficient of a N-monomer aggregate in the continuum regime, $f_N(0)$, is calculated from the creeping flow Stokes equations

$$f_N(Kn = 0) = 6\pi\mu R_m(Kn = 0), \quad [1]$$

where the dependence on the Knudsen number is explicitly shown, and μ is the dynamic gas viscosity. The transition regime friction coefficient, $f_N(Kn)$, may be expressed via the continuum friction coefficient modified empirically by the slip correction factor, $C_N(Kn)$ (Friedlander 2000),

$$f_N(Kn) \equiv \frac{f_N(0)}{C_N(Kn)}. \quad [2]$$

The slip correction factor (hereafter referred to as slip factor) corrects the continuum friction coefficient for velocity-slip effects on the particle surface. For a spherical monomer in the slip-flow regime, Knudsen numbers in the range $0.001 < Kn < 0.25$, the slip correction factor may be analytically calculated (Ivchenko et al. 2007)

$$C_1(Kn) \equiv \frac{f_1(0)}{f_1(Kn)} = \frac{1 + 3c_m Kn}{1 + 2c_m Kn} \quad [3]$$

where c_m is the isothermal slip velocity coefficient. The slip factor can also be calculated via the empirical Knudsen-Weber formula over the entire transition regime (Friedlander 2000),

$$C_1(Kn) = 1 + Kn\left[a + b\exp\left(-\frac{c}{Kn}\right)\right]. \quad [4]$$

Parameters a, b, and c are experimentally-determined and depend on the particle chemical composition (Allen and Raabe 1985). Equation (4) refers to a single sphere, the Knudsen numbers defined for spherical particles (i.e., $Kn = \lambda/R_1$). Hence, its use for more complex structures requires that they be described by an equivalent virtual sphere.

Aerosol particle morphology is usually described by fractal theory (Mandelbrot 1982), a theory applicable to self-similar objects. Studies have shown that even aggregates with small number of monomers obey power-law scaling (di Stasio et al. 2002). Since the scaling law

$$N = k_L\left(\frac{L}{R_1}\right)^{d_L}, \quad [5]$$

holds for a limited range of length scales such aggregates are referred to as power-law or fractal-like aggregates. In Equation (5) N is the number of monomers, k_L a prefactor which depends on the local aggregate structure (Melas et al. 2014a), d_L an exponent, and L an aggregate characteristic length scale. When the characteristic length is geometric $d_L = d_f$, where d_f is the fractal dimension. The most commonly used geometric length scale is the radius of gyration, R_g, the corresponding prefactor being the fractal prefactor, k_f. The radius of gyration is calculated in this work via the definition of Melas et al. (2014a).

The scaling law can be rewritten for dynamic characteristic lengths like the mobility radius (Schmidt-Ott 1988),

$$N = k_m\left(\frac{R_m}{R_1}\right)^{d_m}, \quad [6]$$

where k_m is the mobility prefactor and d_m the mobility fractal dimension. The mobility prefactor and the fractal dimension differ from the fractal prefactor and dimension, but they are related (Sorensen 2011).

The importance of aerosol particle characterization motivated many studies to measure the mobility radius in the transition regime, see, for example, the review by Sorensen (2011). Fractal-like aggregates are classified according to their mobility radii with a differential mobility analyzer (DMA). To obtain information on aggregates' morphology, DMA is used in tandem with other measurement techniques; for example, *in situ* aerodynamic radius measurement with an electrical low pressure impactor (Virtanen et al. 2004) and *ex situ* image analysis with TEM images. Research on aerosol characterization with different techniques is still in progress due to the complexity of relating different aggregate length scales.

In contrast, theoretical studies of particle mobility in the transition regime are much less numerous. To our knowledge, the only theory applicable over the entire transition regime is the Adjusted-Sphere Method (ASM) introduced by Dahneke (1973) and more recently used by Hogan and co-workers (Thajudeen et al. 2012; Zhang et al. 2012). Accordingly, a virtual adjusted sphere is posited to exist, whose radius R_{adj} is constant and independent of flow conditions. The adjusted sphere is defined as a sphere that has the same slip factor as the aggregate over the entire transition regime,

$$f_N(Kn) \equiv \frac{f_N(0)}{C_1(Kn_{\text{adj}})}, \quad \text{with} \quad Kn_{\text{adj}} = \frac{\lambda}{R_{\text{adj}}} = Kn\frac{R_1}{R_{\text{adj}}}, \quad [7]$$

where Kn_{adj} is the adjusted-sphere Knudsen number. It has been applied to geometric objects (Dahneke 1973), straight chains (Dahneke 1982), and fractal-like aggregates (Zhang et al. 2012), while different authors have used it to analyze experimental results (Rogak and Flagan 1992; Shapiro et al. 2012).

The proper hydrodynamic radius of an aggregate is the equivalent mobility radius. In the transition regime, the friction coefficient is expressed as

$$f_N(Kn) = \frac{6\pi\mu R_m(Kn)}{C_1(Kn_m)}, \quad [8]$$

where $C_1(Kn_m)$ is the slip factor of a sphere that has the same mobility as the aggregate, and the mobility Knudsen number is $Kn_m \equiv \lambda / R_m$.

The objective of this study is twofold: first, to determine the effect of particle size on aggregate mobility; second, to relate structural to dynamic properties. We use two different methodologies, the Collision Rate Method (CRM) and the ASM to calculate an aggregate's mobility properties (friction coefficient). According to the CRM, the slip factor, the ratio of two friction coefficients, is related to the ratio of effective collision rates of fictitious Brownian particles. The effective collision rates are obtained from a solution of the Laplace equation with an appropriate boundary condition. The fractal-like aggregates we use are synthetic since they were generated with an algorithm that constructs aggregates with specific properties, independently of an agglomeration mechanism. We calculated the adjusted-sphere radius of different aggregates using the CRM and the results are in excellent agreement with those of ASM. Moreover, for aggregates of known morphology (number of monomers, fractal dimension and prefactor) we calculated the mobility radius. This characterization of aggregate mobility may be viewed as a direct investigation of how morphology determines mobility, to be contrasted to the inverse problem dealt with in experimental studies, whereby information on morphology is extracted from mobility measurements.

2. SLIP CORRECTION FACTOR

2.1. Collision Rate Method (CRM)

Isella and Drossinos (2011) argued that the solution of the Laplace equation may be used to calculate approximately ratios of friction coefficients of straight chains in the continuum regime. Their heuristic argument was motivated by experimental measurements of mass transfer coefficients to nanoparticles of a variety of species, shapes, and sizes (for a review; Keller et al. 2001). The measurements suggested an "empirical scaling law" whereby the product of the mobility of a particle times the mass transfer coefficient is approximately constant. It was interpreted by appealing to the particle active surface area, the surface area upon which mass, momentum, and energy are transferred from the gas to the particle. Since the mass transfer coefficient is proportional to the particle active surface area, and particle mobility is inversely proportional to it, their product is constant. Thus, the mass transfer coefficient is proportional to the friction coefficient (since in the Stokes regime mobility is inversely proportional to the friction coefficient).

The suggested computational methodology mimics the experimental procedure. If multiple scattering events are neglected, the mass transfer coefficient is proportional to the effective collision rate (Rogak et al. 1991). The proportionality constant may be eliminated by taking appropriate collision rate ratios. Therefore, according to the computational procedure proposed by Isella and Drossinos (2011), the friction coefficient of straight chains may be obtained via the calculation of *effective* collision rates of diffusing *fictitious* particles. The fictitious particles behave as Brownian particle in a background gas. Thus, the effective collision rate may be calculated by solving the Laplace equation for the density of the fictitious Brownian particles.

A similar result, in that the scalar, orientationally-averaged friction coefficient of arbitrarily-shaped Brownian particles in the continuum regime was obtained from the solution of the Laplace equation, had been derived analytically by Hubbard and Douglas (1993). Hogan and coworkers (Thajudeen et al. 2012; Zhang et al. 2012) used an alternative approach to solve the diffusion equation via Brownian dynamics simulations of point mass particles to determine the friction coefficient of power-law aggregates across the entire transition regime.

The CRM was validated for straight chains ($d_f = 1, k_f = \sqrt{3}$) (Isella and Drossinos 2011) and then applied to fractal-like aggregates to determine their continuum-regime mobility radius (Melas et al. 2014a). The validity of the CRM was extended to the slip-flow and transition regimes in Melas et al. (2014b). It was argued that the ratio of the friction coefficients in the continuum and the transition regimes equals the ratio of the corresponding fictitious particle-aggregate collision rates,

$$\frac{K_N(0)}{K_N(Kn)} = \frac{f_N(0)}{f_N(Kn)} \equiv C_N(Kn). \qquad [9]$$

where K_N is the collision rate of the Brownian fictitious particles with the N-monomer aggregate.

The effective collision rates are calculated from the Laplace equation $[\nabla^2 \rho(\mathbf{r}) = 0]$, by integrating the fictitious-particle diffusive flux $\mathbf{J}_N = -D_p \nabla \rho$ over the aggregate surface S, where D_p is the fictitious-particle diffusion coefficient and ρ the number density of the fictitious Brownian particles. The appropriate boundary condition far from the aggregate, in both regimes, is constant number density, ρ_∞. On the aggregate surface the fictitious-particle density is specified by

$$\rho(\mathbf{r}_S) = \alpha(Kn)(\hat{\mathbf{n}} \cdot \nabla)\rho\big|_{\mathbf{r}=\mathbf{r}_S}, \qquad [10]$$

where $\mathbf{r}_S$ defines the aggregate surface. The boundary condition is reminiscent of the standard slip-flow boundary condition (Ezquerra Larrodé et al. 2000); it is referred to as the Robin (or radiation) condition. Essentially, rarefaction effects are relegated to the boundary condition. The scaling factor $\alpha(Kn)$, introduced through the boundary condition, is assumed to depend only on the flow regime via the Knudsen number; for $Kn = 0$ it equals zero. It defines a fictitious, extrapolated boundary, internal to the aggregate, where the boundary condition at $\mathbf{R} = \mathbf{r}_S - \alpha \hat{\mathbf{n}}$ is Dirichlet and the density is zero.

The fictitious Brownian particle-monomer effective collision rate in slip-flow is obtained from the analytical solution of the

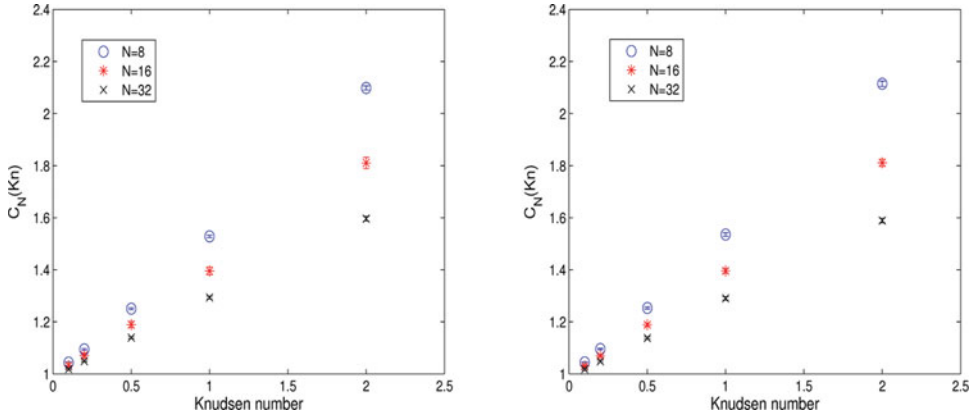

FIG. 1. Slip factor of DLCA (left) and RLCA (right) aggregates calculated with CRM, averaged over ten aggregate realizations. Error bars denote the standard deviation.

Laplace equation in spherical coordinates

$$K_1(Kn) = K_1(0)\left(1+\frac{\alpha}{R_1}\right)^{-1}, \quad \text{with} \quad K_1(0) = 4\pi D_p R_1 \rho_\infty. \tag{11}$$

If we combine Equations (9) and (11), we obtain that α(Kn) is determined from the monomer slip factor

$$\frac{\alpha}{R_1} = \frac{K_1(0)}{K_1(Kn)} - 1 = C_1(Kn) - 1. \tag{12}$$

It can be easily calculated using either the analytical expression, Equation (3), or the Knudsen-Weber formula, Equation (4) for the slip factor.

We calculated the slip factor of fractal-like aggregates using the CRM. They were created with a tunable cluster–cluster aggregation algorithm (Filippov et al. 2001). It is not based on a physical agglomeration mechanism, but it allows the generation of aggregates that have prescribed number of primary particles, fractal dimension and prefactor. In addition, they satisfy exactly the scaling law. The generated aggregates are composed of equal-sized, spherical, non-overlapping monomers. Moreover, these aggregates share many features with aggregates generated by physical process-based algorithms. A detailed description of the algorithm and the properties of the aggregates it generates can be found in a previous work (Melas et al. 2014a).

The CRM validity is limited to the slip flow regime, but it was empirically found that it may be extended up to monomer $Kn = 2$ for straight chains (Melas et al. 2014b). The determination of the scaling factor $\alpha(Kn)$ for a given Kn is done via Equation (12). The monomer slip correction factor is specified by the Knudsen-Weber formula, Equation (4). The monomer-slip factor parameters used were those proposed by Allen and Raabe (1985) for an accommodation coefficient 0.763 ($a = 1.142, b = 0.558, c = -0.999$). For the numerical simulations we used the finite-element software COMSOL Multiphysics 4.0a (COMSOL 2010). We ensured that the computational domain was large enough to impose the boundary condition away from the aggregate surface, and that further mesh refinement did not alter significantly our results. The simulations were performed in scaled units ($\rho_\infty = 1$, $D_p = 1$, and $R_1 = 1$).

The simulated aggregates were composed of $N = [8, 16, 32]$ monomers. The fractal dimension and prefactor (d_f, k_f) were (1.8, 1.3) and (2.05, 0.94) that correspond to aggregates generated by diffusion limited cluster aggregation (DLCA) and reaction limited cluster aggregation (RLCA), as recommended by Brasil et al. (2000) and Lattuada et al. (2003), respectively. The results were averaged over 10 different aggregate realizations for each number of monomers: in total 30 DLCA and 30 RLCA aggregates were analyzed. Figure 1 presents the calculated slip factor (averaged over 10 aggregate realizations) and the standard deviation as a function of monomer Knudsen number. The standard deviation is not easily visible as it is very small; its maximum value is 1.19% (DLCA) and 0.75% (RLCA). These results suggest that a unique slip factor, and consequently friction coefficient, corresponds to a specific $(N, d_f, k_f; Kn)$.

The slip factors plotted in Figure 1 can be used to calculate the adjusted-sphere radius R_{adj} that, according to Equations (2) and (7) satisfies

$$C_N(Kn) \equiv C_1(Kn_{\text{adj}}) = 1 + Kn_{\text{adj}}\left[a + b\exp\left(-\frac{c}{Kn_{\text{adj}}}\right)\right]. \tag{13}$$

Since R_{adj} is the only unknown, the nonlinear transcendental equation may be solved graphically.

We calculated the adjusted-sphere radius of the simulated aggregates in Figure 2. Ten aggregate realizations for each (N, d_f, k_f) for five different Knudsen numbers, Kn = [0.1, 0.2, 0.5, 1, 2], lead to fifty R_{adj}. Figure 2 presents the scaled (on the monomer radius R_1) adjusted-sphere radius, averaged over aggregate realizations, as a function of the Knudsen number. We note a very strong dependence of R_{adj}/R_1 on the monomer Knudsen number for $Kn < 0.5$, becoming much

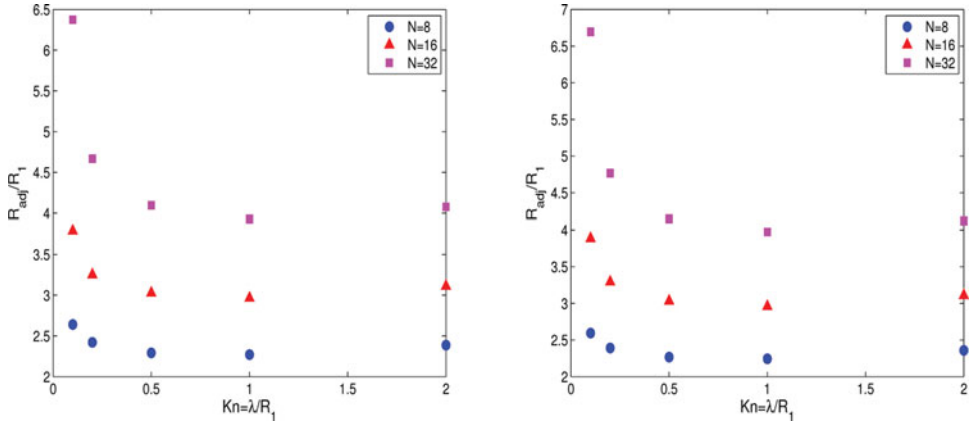

FIG. 2. Dimensionless adjusted-sphere radius of DLCA (left) and RLCA (right) aggregates calculated with the CRM, averaged over ten aggregate realizations.

weaker for $0.5 \leq Kn \leq 2.0$. A similar dependence of the adjusted-sphere radius on flow conditions, as specified by λ, was also observed for straight chains (Melas et al. 2014b). Even though as $Kn \to 0$ the numerical solution of Equation (13) becomes difficult, in that small changes of $C_N(Kn)$ lead to large changes of R_{adj}, numerical instabilities do not seem sufficient to justify such a strong effect at small Knudsen numbers.

The adjusted-sphere radius dependence on Kn, as determined by the CRM, seems to be in contrast to the main assumption of the ASM. However, its variation for $0.5 \leq Kn \leq 2.0$ is relatively small. Figure 3 presents the average dimensionless adjusted-sphere radii of DLCA (left) and RLCA (right) aggregates and the standard deviation as a function of number of monomers. The average was calculated over $Kn = [0.5, 1, 2]$; it is denoted by angular brackets.

The maximum standard deviation is 4.3% (DLCA) and 3.2% (RLCA), suggesting that the average, over Knudsen numbers, adjusted-sphere radius is relatively well defined. This average, independent of the Knudsen number, may be associated with the aggregates. It becomes the characteristic length scale to be used in the calculation of the slip factor over the entire transition regime, as the ASM posits. In that sense, the triplet (N, d_f, k_f) defines a unique (averaged over a range of Knudsen numbers) R_{adj}/R_1 that is approximately flow independent, and may be considered an approximate geometric descriptor of that aggregate.

2.2. Adjusted Sphere Method (ASM)

The adjusted-sphere Knudsen number may be calculated by (Rogak and Flagan 1992)

$$Kn_{\text{adj}} = Kn \frac{R_1 R_m(0)}{R_m^2(\infty)}, \qquad [14]$$

where $R_m(\infty)$ is the mobility radius in the free molecular regime. The derivation of Equation (14) was described in previous works (Zhang et al. 2012; Melas et al. 2014b). It shows that the calculation of the continuum and free molecular mobility radii are sufficient to obtain the adjusted-sphere Knudsen number, and consequently the slip factor via the Knudsen-Weber formula.

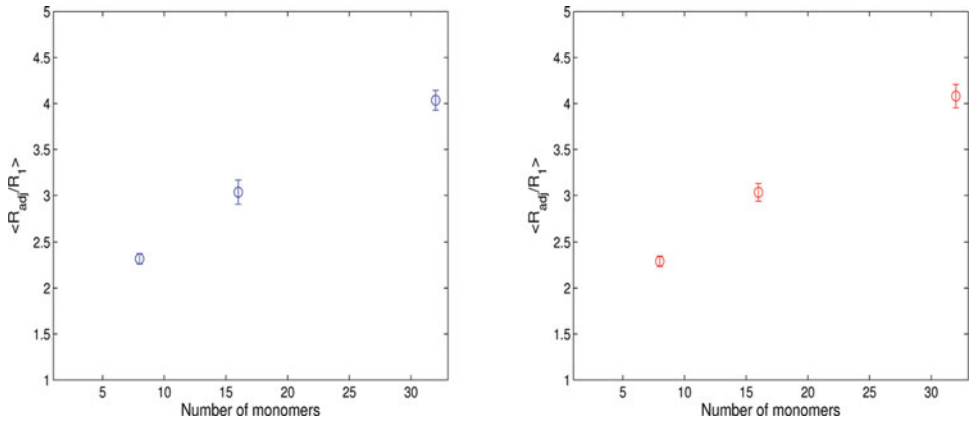

FIG. 3. Average, over three Knudsen numbers, adjusted-sphere radius of DLCA (left) and RLCA (right) aggregates calculated with the CRM. Error bars denote the standard deviation.

2.2.1. *Continuum-Regime Mobility Radius*

The continuum-regime mobility radius of aggregates generated by the algorithm used in this study has been calculated via the CRM (Melas et al. 2014a). Its connection to structural properties was studied to determine that for a given number of monomers, a linear relationship exists between the mobility radius and the radius of gyration,

$$\frac{R_m(0)}{R_1} = 0.248(2 - N^{-1/3})\frac{R_g}{R_1} + 0.69N^{0.415}. \qquad [15]$$

Equation (15) shows that the mobility radius depends on both the fractal dimension and prefactor in the particular combination that defines the radius of gyration R_g. It, also, depends explicitly on the monomer radius R_1. Equation (15), and the numerical fits proposed in the following sections, contain the factor $N^{1/3}$: they may equally well be expressed in terms of the equivalent volume radius, $R_{eq}/R_1 = N^{1/3}$, the radius of a sphere that has the same volume as the aggregate.

2.2.2. *Orientationally-Averaged Projected Area*

In the free molecular regime, the friction coefficient is proportional to the squared mobility radius according to the kinetic theory of gases (Cai and Sorensen 1994). Moreover, the mobility radius is proportional to the orientationally-averaged projected area A_p of the aggregate

$$\frac{R_m^2(\infty)}{R_1^2} = \frac{A_p}{\pi R_1^2}. \qquad [16]$$

The orientationally-averaged projected area of several aggregates was calculated as follows. The minimum rectangle that encloses an aggregate's projected area was designed and calculated (A_{rect}); Monte Carlo sampling was used to determine the projected area: 10^5 points on the rectangle were checked whether they belonged to the aggregate's projection, N_{pr}, or not, $N_{\text{total}} - N_{pr}$. The calculated random projected area is

$$A_p = \frac{N_{pr}}{N_{\text{total}}} A_{\text{rect}}. \qquad [17]$$

Two different methods were used. According to the first method, a randomly chosen projected area of an aggregate with specific (N, d_f, k_f) was calculated, and then averaged over 5000 different aggregates. We calculated the projected area of aggregates consisting of 8, 16, 32, and 64 monomers with (d_f, k_f) in the ranges ([1.5, 2.1], [1, 1.6]). These aggregates had been used in a previous work (Melas et al. 2014a). Figure 4 plots the average projected area against the squared radius of gyration.

For a given number of monomers a linear relationship exists between the logarithm of the projected area and the logarithm of the squared radius of gyration. For fixed N we fit linearly the data: both the slope and the intercept are functions of N. They

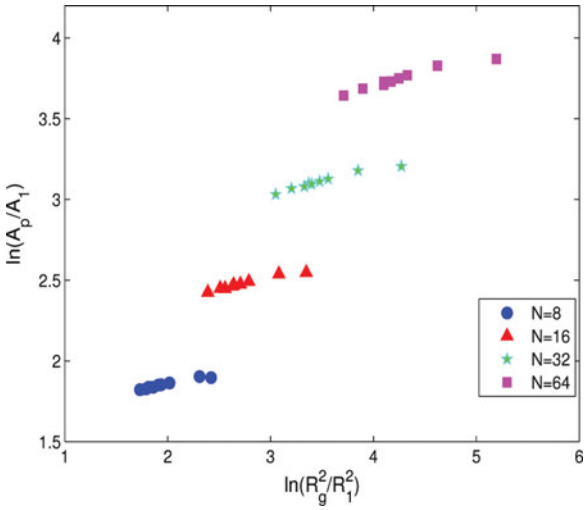

FIG. 4. Orientationally-averaged projected area of 5000 aggregates for each triplet (N, d_f, k_f), against their squared radius of gyration. The (d_f, k_f) range is ([1.5 − 2.1, 1 − 1.6]).

are averaged to obtain the empirical fit

$$\frac{A_p}{A_1} = 1.172\, N^{0.704} \left(\frac{R_g}{R_1}\right)^{2(-0.146N^{-1/3}+0.192)}, \qquad [18]$$

where A_1 is the projected area of a sphere, $A_1 = \pi R_1^2$. According to the second method, the projected area of a single aggregate was averaged over 5000 random projections.

Figure 5 shows the average projected area of 10 DLCA and RLCA aggregates as a function of number of monomers. The maximum standard deviation is 0.8% (DLCA) and 1.1% (RLCA). It also compares projected areas calculated with the second method to our numerical fit: the agreement is excellent with a maximum deviation 1.3% (DLCA) and 1.6% (RLCA). Moreover, we compare Equation (18) to previously reported expressions (Mackowski 2006; Sorensen 2011; Thajudeen et al. 2012). These expressions are reproduced in the online supplemental information, where, in addition, we present probability distributions of scaled projected areas of four DLCA and RLCA 32-monomer aggregates.

Thajudeen et al. (2012) calculated the orientationally-averaged projected area of aggregates generated with an algorithm similar to ours; they also used Monte Carlo sampling. They suggested a seven parameter fit, valid for constant $k_f = 1.3$ and d_f in the range [1.3–2.6]. For DLCA aggregates, the two fits are in very good agreement, the maximum difference being 2%.

Our calculations are also compared to an expression proposed by Sorensen (2011) for the free molecular mobility radius of DLCA aggregates as a function of number of monomers. The maximum difference of these results from the mobility radius calculated via the projected-area expression is 6.5%.

Mackowski (2006) generated fractal-like aggregates with a mimicking algorithm similar to the algorithm used herein. He

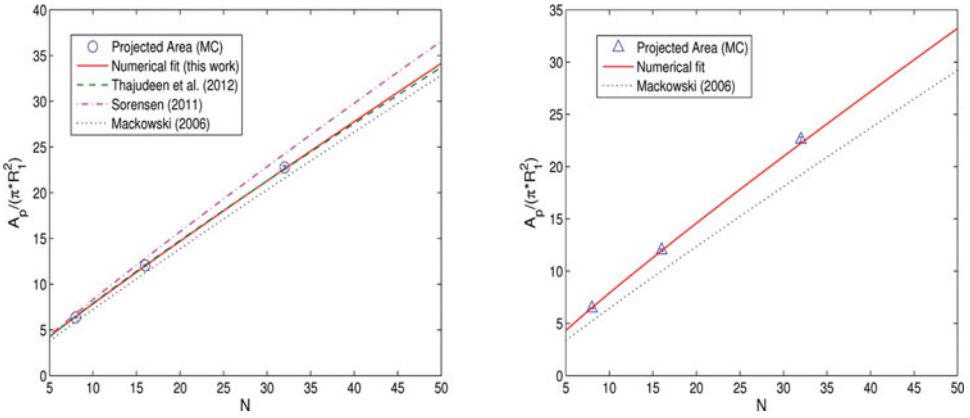

FIG. 5. Orientationally-averaged projected area of 10 DLCA (left) and RLCA (right) aggregates. The error bars denote the standard deviation. Comparison of proposed numerical expression and literature values.

calculated the hydrodynamic drag using a Monte Carlo technique, and he proposed an expression for the free molecular mobility radius valid for a range of fractal dimensions and prefactors: $d_f = [1.7–2]$, $k_f = [0.7–2.2]$ and N up to 3000. We used it to calculate the squared free molecular mobility radius of both DLCA and RLCA aggregates, even though the d_f of RLCA aggregates is slightly beyond the region of validity of the proposed expression. The two numerical expressions for DLCA (RLCA) aggregates differ by a maximum of 7.8% (18%).

2.2.3. *Adjusted-Sphere Radius*

The combination of the expressions for the adjusted-sphere Knudsen numbers Equations (7) and (14) allows the direct calculation of the adjusted-sphere radius from the continuum and free molecular mobility radii,

$$\frac{R_{\text{adj}}}{R_1} = \frac{A_p}{\pi R_1 R_m(0)} = \frac{R_m^2(\infty)}{R_1 R_m(0)}. \qquad [19]$$

Figure 6 presents the adjusted-sphere radius against the radius of gyration of aggregates composed of $N = [10,60]$ monomers and (d_f, k_f) in the range ([1.5, 2.1],[1, 1.6]). The adjusted-sphere radius is calculated by substituting the numerical expressions Equations (15) and (18) into Equation (19).

As in the case of the continuum-regime mobility radius and the orientationally-averaged projected area, the adjusted-sphere radii cluster according to the number of monomers. We follow a similar procedure to fit our data: for a fixed number of monomers they are fitted linearly, then the six slopes and intercepts (one for each N) are averaged to obtain an expression that reproduces our data with less than 1% error,

$$\frac{R_{\text{adj}}}{R_1} = -0.052(2 + N^{-1/3})\frac{R_g}{R_1} + 1.15N^{0.42}. \qquad [20]$$

Thus, the adjusted-sphere radius may be estimated using non-ensemble averaged properties, the number of monomers and the radius of gyration. It shows the importance of both (d_f, k_f), which, even though not individually needed, they determine the radius of gyration. Note that all three numerical expressions we propose, Equations (15), (18), and (20), suggest that unique $R_m(0)/R_1$, A_p/A_1, and R_{adj}/R_1 correspond to a unique triplet (N, d_f, k_f), but not vice versa.

2.3. Comparison of Different Methods

We investigate whether the CRM and the ASM lead to the same slip factor. Figure 7 presents the slip factor of DLCA (left) and RLCA (right) aggregates against the Knudsen number over the entire transition regime. With squares we plot the slip factor averaged over 10 aggregate realization for each N, calculated by combining the CRM with the ASM; namely, R_{adj}/R_1 is calculated via CRM and then substituted in the Knudsen-Weber formula. We refer to this methodology as modified CRM. The Knudsen-Weber parameters used in all our calculations are

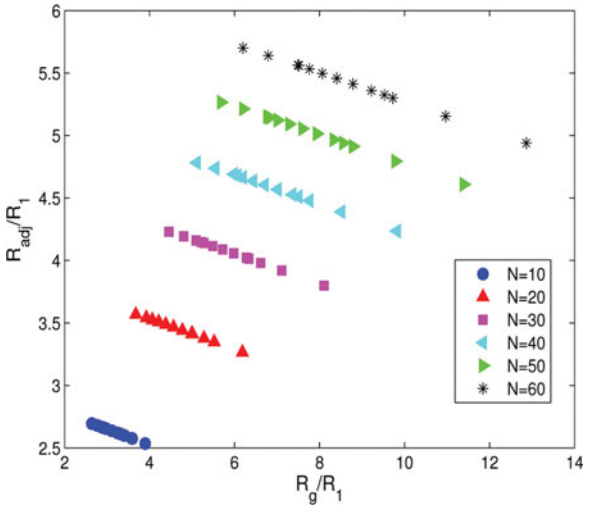

FIG. 6. The adjusted-sphere radius calculated with the ASM, Equation (19), against the radius of gyration. The (d_f, k_f) range is [1.5–2.1, 1–1.6].

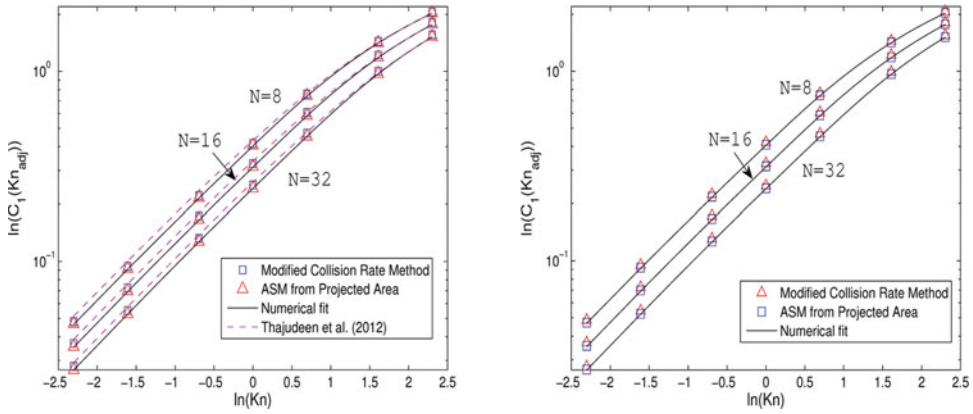

FIG. 7. Slip correction factor of DLCA (left) and RLCA (right) aggregates calculated via the modified CRM, the ASM, and comparison of the proposed numerical fit, Equation (20), to a previously reported expression (left).

those proposed by Allen and Raabe (1985). With triangles we plot the average slip factor of the same aggregates calculated with the ASM. Accordingly, the continuum mobility radius is calculated with the CRM, whereas the free molecular mobility radius is obtained from the average of 5000 different projections of each aggregate (Equations (16) and (18); Figure 5). The resulting radii are substituted into Equation (14) to determine the adjusted-sphere Knudsen number and the slip factor. The agreement between the two different methods, CRM and ASM, is excellent as the difference never exceeds 3.5%.

With solid lines we plot the slip factors calculated using the numerical expression for the adjusted-sphere radius, Equation (20). Our numerical fit predictions are in good agreement with the ASM and the CRM data, 0.9% and 4.4% maximum error, respectively. Thajudeen et al. (2012) used the ASM to calculate the slip factor of fractal-like aggregates. They proposed numerical fits for the continuum and free molecular mobility radii which substituted into Equation (14) give the slip factor. We compare their predictions for DLCA aggregates: the difference never exceeds 2.9%. Note that Thajudeen et al. (2012) used the Knudsen-Weber formula parameters proposed by Davies (1.257, 0.4, −1.1). Figure 7 shows that both CRM and ASM calculate almost identical slip factors. Hence, slip factors calculated via a constant R_{adj}/R_1, as postulated by the ASM, and via $\langle R_{adj}\rangle/R_1$ by averaging over Knudsen numbers, as used by the modified CRM, are in very good agreement.

It is worthwhile to compare R_{adj}/R_1 calculated as prescribed by the ASM, that is, via Equation (19), and via the CRM, that is, by averaging calculated radii over (three) Knudsen numbers, $\langle R_{adj}\rangle/R_1$. Table 1 presents this comparison. In agreement with the results shown in Figure 7, the adjusted-sphere radii calculated via two different methods are in relatively good agreement, differing at maximum by approximately 4%. Hence, either method may be used to calculate the slip factor, and an approximately constant, flow-independent, geometric length scale may be associated with a fractal-like aggregate.

3. MOBILITY RADIUS IN THE TRANSITION REGIME

3.1. Relationship Between the Mobility Radius and the Radius of Gyration

From the two definitions of the transition-regime friction coefficient, Equations (7) and (8), we obtain

$$\frac{R_m(0)}{C_1(Kn_{adj})} = \frac{R_m(Kn)}{C_1(Kn_m)}. \qquad [21]$$

TABLE 1
Comparison of adjusted-sphere radii: averaged over three Knudsen numbers, $\langle R_{adj}\rangle$, and via the numerical expression Equation (19), R_{adj}

N	DLCA $\langle R_{adj}\rangle/R_1$ (CRM)	R_{adj}/R_1 (ASM)	Difference %	RLCA $\langle R_{adj}\rangle/R_1$ (CRM)	R_{adj}/R_1 (ASM)	Difference %
8	2.32	2.38	2.55	2.29	2.37	3.30
16	3.03	3.16	3.99	3.03	3.16	4.08
32	4.03	4.20	4.21	4.08	4.23	3.79

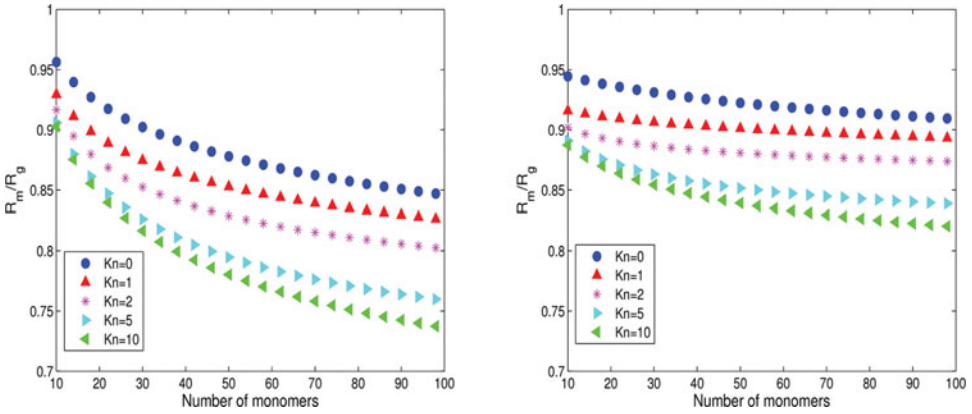

FIG. 8. Ratio of the mobility radius to the radius of gyration for different Knudsen numbers. Left: DLCA aggregates; right: RLCA aggregates.

Thus, it is sufficient to calculate the continuum-regime mobility radius and the adjusted-sphere slip factor to obtain the mobility radius. The continuum-regime mobility radius, as calculated by CRM, is approximately given by Equation (15). The slip correction factor may be calculated either with the CRM or with the ASM. We choose the ASM, and, more specifically, the numerical fit Equation (20) that permits a faster calculation for a wide range of (N, d_f, k_f) and Knudsen numbers. The mobility radius is obtained by solving the nonlinear Equation (21) graphically.

Figure 8 presents the ratio of the mobility radius to the radius of gyration of DLCA (left) and RLCA (right) aggregates as a function of the number of monomers, for $Kn = [0, 1, 2, 5, 10]$. This ratio is occasionally taken to be constant, flow independent. Instead, we find that for DLCA aggregates it depends on both the number of monomers and the Knudsen number. As the number of monomers and the Knudsen number increase the ratio tends to decrease. For large number of monomers, it seems to tend to a constant. For RLCA aggregates the ratio depends mainly on the Knudsen number, with a weaker dependence on the number of monomers. Previous studies (Filippov 2000) also noted a weak dependence on the Knudsen number, even for the small Knudsen numbers considered.

Equation (21), which shows that the mobility radius is a function of the Knudsen number, in conjunction with the dependence of $R_m(0)/R_1$ on (N, d_f, k_f) suggests that the functional dependence of the mobility radius in the transition regime may be expressed as $R_m(N, d_f, k_f; Kn; R_1)$. Note that we included the explicit dependence of the mobility radius on R_1.

3.2. Mobility Scaling Law

The mobility fractal dimension and prefactor may be calculated by plotting the logarithm of the number of monomers against the logarithm of the mobility radius for an ensemble of aggregates that have the same (d_f, k_f). We generated these plots for DLCA and RLCA aggregates. The resulting scaling-law parameters for different Knudsen numbers are presented in Table 2. The number of monomers was in the range $N \in [10, 100]$. The pair (d_m, k_m) depends weakly on the Knudsen number. More specifically, d_m tends to increase as the Knudsen number increases, while k_m increases up to $Kn = 2$ and then decreases. Note that $(d_f, k_f) \neq (d_m, k_m)$.

The (d_m, k_m) we calculate for the continuum regime RLCA aggregates differ slightly from those presented in a previous work (Melas et al. 2014a) where simulations were performed for N up to 1000. They differ because the pair (d_m, k_m) depends weakly on the number of monomers. We chose a small monomer number because combustion-generated aggregates are usually composed of few decades of monomers.

Our results compare favorably to experimental results. Schmidt-Ott (1988) measured the mobility fractal dimension of silver aggregates using aerosol photoemission. The primary particle size was 7.5 nm. Since the gas mean free path is approximately 65 nm (under usual atmospheric conditions), $Kn = 8.7$. The d_m he proposed was 2.18. Maricq and Xu (2004) used a tandem DMA and an electric low pressure impactor to measure $d_m = 2.15 \pm 0.1$ for flame-generated soot and $d_m = 2.3 \pm 0.1$ for diesel exhaust particulate matter. Sorensen (2011) reports that in the transition regime d_m remains constant. The range of values that he provides for DLCA aggregates are slightly larger than ours, $d_m = 2.22 \pm 0.1$. In a recent study, Mamakos et al.

TABLE 2
Mobility fractal dimension and prefactor of DLCA and RLCA aggregates for different Knudsen numbers

Kn	(d_m, k_m) DLCA	(d_m, k_m) RLCA
0	(1.97,1.17)	(2.11,0.98)
1	(1.98,1.23)	(2.10,1.07)
2	(2,1.25)	(2.11,1.10)
5	(2.09,1.17)	(2.17,1.06)
10	(2.14,1.11)	(2.21,1.02)
∞	(2.17,1.08)	(2.22,1.02)

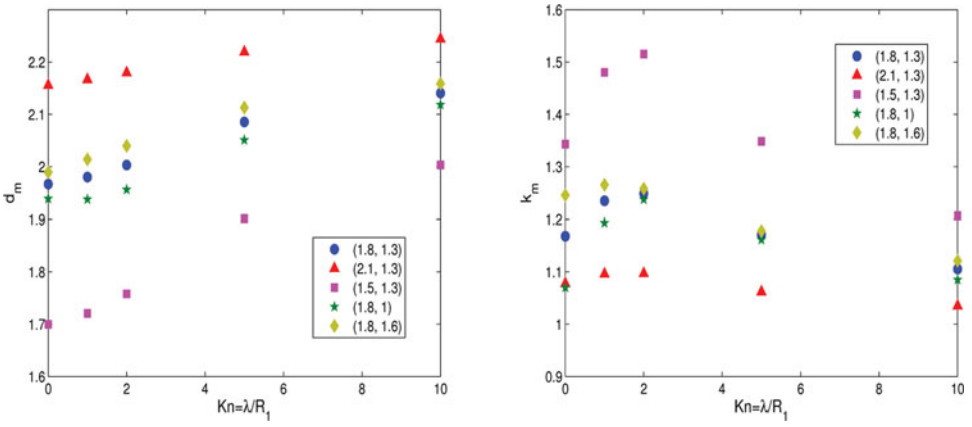

FIG. 9. Mobility fractal dimension, d_m, and prefactor, k_m, of aggregates characterized by different pairs (d_f, k_f).

(2013), generated soot particles with a mini-CAST burner that were treated in a Catalytic Stripper. The primary particle size was between 8.5 nm and 34 nm, which corresponds to $Kn = 7.6$ and 1.9, respectively. They used an experimental setup similar to Maricq and Xu (2004) and they determined the mobility fractal dimension to be $d_m = 2.1 - 2.25$.

We study the effect of the fractal dimension and prefactor on the mobility fractal dimension and prefactor in Figure 9. It presents the mobility fractal dimension (left) and the mobility fractal prefactor (right) as a function of the Knudsen number. The simulated aggregates had either constant $k_f = 1.3$ and varying fractal dimensions, or constant $d_f = 1.8$ and varying fractal prefactors.

The mobility fractal dimension increases for increasing Knudsen number. This behavior is the same for all pairs of (d_f, k_f). Instead, the mobility fractal prefactor increases up to $Kn = 2$ and then decreases. When d_f increases d_m increases. Moreover, changes of k_f result in changes to both (d_m, k_m), especially for $Kn \leq 2$. Hence, the pair (d_m, k_m) depends on the pair (d_f, k_f).

4. HYDRODYNAMIC RADIUS AND DYNAMIC SHAPE FACTOR

The hydrodynamic radius is defined as the radius of a sphere that has the same average mobility in the continuum regime as the aggregate at a given Knudsen number,

$$f_N(Kn) \equiv 6\pi\mu R_h(Kn). \quad [22]$$

Accordingly, the hydrodynamic radius is proportional to the friction coefficient, and $R_h(0) = R_m(0)$. By combining Equations (8) and (22), we obtain $R_h(Kn) = R_m(Kn)/C_1(Kn_m)$. Since the mobility radius has been calculated, and the slip factor $C_1(Kn_m)$ is easily obtained via the Knudsen-Weber formula, the hydrodynamic radius may be calculated.

Figure 10 presents calculated hydrodynamic radii for DLCA (left) and RLCA (right) aggregates as a function of monomer number. The hydrodynamic radius, and consequently the friction coefficient, depends strongly on the monomer Knudsen number: for increasing Knudsen number it decreases. Moreover, it depends on the number of monomers.

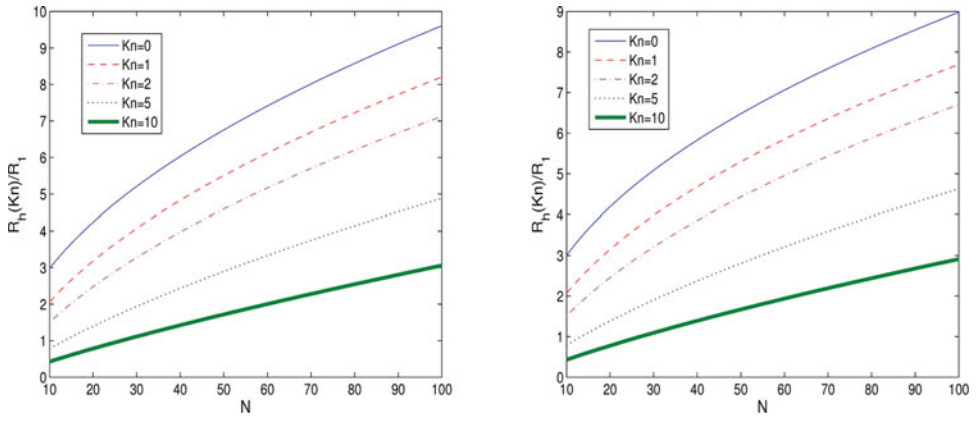

FIG. 10. The hydrodynamic radius of DLCA (left) and RLCA (right) aggregates for different monomer Knudsen numbers as a function of the number of monomers.

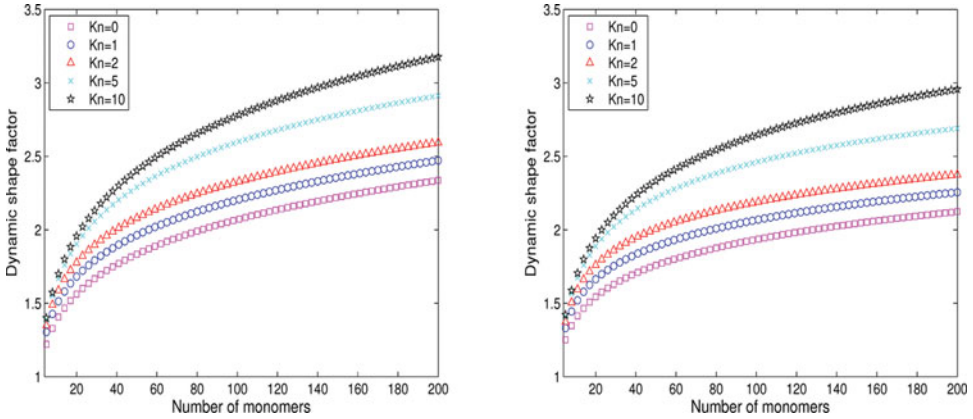

FIG. 11. Dynamic shape factor for different Knudsen numbers as a function of number of monomers. Left: DLCA clusters; right: RLCA clusters.

Another quantity associated with irregularly-shaped particles is the dynamic shape factor, χ_N, a correction factor used to account for the effect of the aggregate shape on its motion. The transition regime friction coefficient can be expressed as

$$f_N = \frac{6\pi\mu\chi_N(Kn)\,R_{eq}}{C_1(Kn_{eq})} \qquad [23]$$

In the continuum regime, the dynamic shape factor is $\chi_N(0) = R_{eq}/R_m(0)$ (Isella and Drossinos 2011). In the transition regime

$$\chi_N(Kn) = \frac{R_m(0)}{C_1(Kn_{\text{adj}})}\frac{C_1(Kn_{eq})}{R_{eq}} = \chi_N(0)\frac{C_1(Kn_{eq})}{C_1(Kn_{\text{adj}})}, \qquad [24]$$

where Kn_{eq} is the equivalent-volume Knudsen number, $Kn_{eq} = KnR_1/R_{eq}$. We used Equations (15), (20), and (24) to calculate the dynamic shape factor of DLCA (Figure 11, left) and RLCA (right) aggregates. The dynamic shape factor increases as either the number of monomers or the Knudsen number increase. It seems to approach an asymptotic value for increasing number of monomers.

The dynamic shape factor may also be used to obtain the aggregate effective density (ρ_{eff}), the density of a fictitious spherical particle of radius the mobility radius and of the same mass as the initial aggregate,

$$\frac{\rho_{\text{eff}}}{\rho_1} = \left[\frac{C_1(Kn_{eq})}{C_1(Kn_m)}\frac{1}{\chi_N(Kn)}\right]^3, \qquad [25]$$

where ρ_1 is the monomer material density. The effective density is calculated experimentally with combined measurements of aggregate mobility and aerodynamic radii of aggregates (Mamakos et al. 2013).

5. CONCLUSIONS

The objective of our study was to investigate the effect of particle size and morphology on the mobility of power-law aggregates. We applied and compared two different methodologies, the CRM and the ASM, to calculate the friction coefficient and the equivalent mobility radius of synthetic DLCA and RLCA aggregates in the mass and momentum transition regimes.

The CRM is a methodology to calculate the slip correction coefficient of power-law aggregates in the continuum and slip-flow regimes. It relates it to the solution of the Laplace equation with an appropriate boundary condition. The ASM assumes the existence of a constant and flow independent radius, the adjusted-sphere radius, that allows the calculation of the slip factor over the entire Knudsen number range.

Calculated slip correction factors via the CRM and the ASM were found to be in very good agreement. The adjusted-sphere radius, as calculated by CRM, was found to depend weakly on the monomer Knudsen number for $0.5 \leq Kn \leq 2.0$. Its average, over three Knudsen numbers, was in reasonably good agreement with the ASM-calculated adjusted-sphere radius, maximum difference of 4%. Further experimental data or predictive computational studies would be required to confirm this result.

A fractal-like scaling law was found to hold if the characteristic length scale is chosen to be the equivalent mobility radius. The mobility fractal dimension d_m and prefactor k_m were found to depend strongly on aggregate morphology and weakly on the Knudsen number. Both the fractal dimension and prefactor influence the pair (d_m, k_m).

DISCLAIMER

The views expressed in the article are purely those of the authors and may not in any circumstances to be regarded as stating an official position of the European Commission.

SUPPLEMENTAL MATERIAL

Supplemental data for this article can be accessed on the publisher's website.

REFERENCES

Allen, M. D., and Raabe, O. G. (1985). Slip Correction Measurements of Spherical Solid Aerosol Particles in an Improved Millikan Apparatus. *Aerosol Sci. Technol.*, 4:269–286.

Brasil, A., Farias, T., and Carvalho, M. (2000). Evaluation of the Fractal Properties of Cluster-Cluster Aggregates. *Aerosol Sci. Technol.*, 33:440–454.

Cai, J., and Sorensen, C. M. (1994). Diffusion of Fractal Aggregates in the Free Molecular Regime. *Phys. Rev. E*, 50:3397–3400.

COMSOL Multiphysics, (2010). Chemical Engineering Module, Version 4.0a. http://www.comsol.com/products.

Dahneke, B. (1982). Viscous Resistance of Straight-Chain Aggregates of Uniform Spheres. *Aerosol Sci. Technol.*, 1:179–185.

Dahneke, B. E. (1973). Slip correction Factors for Nonspherical Bodies–III The Form of the General Law. *Aerosol Sci.*, 4:163–170.

di Stasio, S., Konstandopoulos, A. G., and Kostoglou, M. (2002). Cluster-Cluster Aggregation Kinetics and Primary Particle Growth of Soot Nanoparticles in Flame by Light Scattering and Numerical Simulations. *J. Colloid Interface Sci.*, 247:33–46.

Ezquerra Larrodé, F., Housiadas, C., and Drossinos, Y. (2000). Slip-Flow Heat Transfer in Circular Tubes. *Int. J. Heat Mass Transfer*, 43:2669–2680.

Filippov, A. V. (2000). Drag and Torque on Clusters of N Arbitrary Spheres at Low Reynolds Number. *J. Colloid Interface Sci.*, 229:184–195.

Filippov, A., Zurita, M., and Rosner, D. (2001). Fractal-Like Aggregates: Relation Between Morphology and Physical Properties. *J. Colloid Interface Sci.*, 229:261–273.

Friedlander, S. K. (2000). *Smoke, Dust and Haze*. 2nd Edition. Oxford University Press, New York.

Giechaskiel, B., Alföldy, B., and Drossinos, Y. (2009). A Metric for Health Effects Studies of Diesel Exhaust Particles. *J. Aerosol Sci.*, 40:639–651.

Hubbard, J. B., and Douglas, J. F. (1993). Hydrodynamic Friction of Arbitrarily Shaped Brownian Particles. *Phys. Rev. E*, 47:R2983–R2986.

Isella, L., and Drossinos, Y. (2011). On the Friction Coefficient of Straight-Chain Aggregates. *J. Colloid Interface Sci.*, 356:505–512.

Ivchenko, I. N., Loyalka, S. K., and Tompson, R. V. (2007). *Analytical Methods for Problems of Molecular Transport*. Springer, DordrechtThe Netherlands.

Kaufman, Y. J., and Koren, I. (2006). Smoke and Pollution Aerosol Effect on Cloud Cover. *Science*, 313:655–658.

Keller, A., Fierz, M., Siegmann, K., Siegmann, H. C., and Filippov, A. (2001). Surface Science with Nanoparticles in a Carrier Gas. *J. Vacuum Sci. Technol. A*, 19:1–8.

Kostoglou, M., and Konstandopoulos, A. G. (2001). Evolution of Aggregate Size and Fractal Dimension During Brownian Coagulation. *J. Aerosol Sci.*, 32:1399–1420.

Lattuada, M., Wu, H., and Morbidelli, M. (2003). Hydrodynamic Radius of Fractal Clusters. *J. Colloid Interface Sci.*, 268:96–105.

Mackowski, D. W. (2006). Monte Carlo Simulation of Hydrodynamic Drag and Thermophoresis of Fractal Aggregates of Spheres in the Free-Molecule Flow Regime. *J. Aerosol Sci.*, 37:242–259.

Mamakos, A., Khalek, I., Giannelli, R., and Spears, M. (2013). Characterization of Combustion Aerosol Produced by a Mini-CAST and Treated in a Catalytic Stripper. *Aerosol Sci. Technol.*, 47:927–936.

Mandelbrot, B. B. (1982). *The Fractal Geometry of Nature*. Freeman, San Francisco, CA.

Maricq, M. M., and Xu, N. (2004). The Effective Density and Fractal Dimension of Soot Particles from Premixed Flames and Motor Vehicle Exhaust. *J. Aerosol Sci.*, 35:1251–1274.

Melas, A. D., Isella, L., Konstandopoulos, A. G., and Drossinos, Y. (2014a). Morphology and Mobility of Synthetic Colloidal Aggregates. *J. Colloid Interface Sci.*, 417:27–36.

Melas, A. D., Isella, L., Konstandopoulos, A. G., and Drossinos, Y. (2014b). Friction Coefficient of Straight Chains over the Entire Knudsen-Number Range. (submitted).

Rogak, S. N., Baltensperger, U., and Flagan, R. C. (1991). Measurement of Mass Transfer to Agglomerate Aerosol. *Aerosol Sci. Technol.*, 14:447–458.

Rogak, S. N., and Flagan, R. C. (1992). Coagulation of Aerosol Agglomerates in the Transition Regime. *J. Colloid Interface Sci.*, 151:203–224.

Schmidt-Ott, A. (1988). New Approaches to in Situ Characterization of Ultrafine Agglomerates. *J. Aerosol Sci.*, 19:553–563.

Shapiro, M., Vainshtein, P., Dutcher, D., Emery, M., Stolzenburg, M., Kittelson, D. B. et al. (2012). Characterization of Agglomerates by Simultaneous Measurement of Mobility, Vacuum Aerodynamic Diameter and Mass. *J. Aerosol Sci.*, 44:24–45.

Sorensen, C. M. (2011). The Mobility of Fractal Aggregates: A Review. *Aerosol Sci. Technol.*, 45:755–769.

Thajudeen, T., Gopalakrishnan, R., and Hogan, Jr, C. J. (2012). The Collision Rate of Nonspherical Particles and Aggregates for all Diffusive Knudsen Numbers. *Aerosol Sci. Technol.*, 46:1174–1186.

Virtanen, A., Ristimaki, J., and Keskinen, J. (2004). Method for Measuring Effective Density and Fractal Dimension of Aerosol Agglomerates. *Aerosol Sci. Technol.*, 38:437–446.

Zhang, C., Thajudeen, T., Larriba, C., Schwartzentruber, T. E., and Hogan, Jr, C. J. (2012). Determination of the Scalar Friction Factor for Nonspherical Particles and Aggregates Across the Entire Knudsen Number Range by Direct Simulation Monte Carlo (DSMC). *Aerosol Sci. Technol.*, 46:1065–1078.